Clays and Clay Minerals, Vol. 69, No. 1:117– 127, 2021

FUNCTIONALIZED HALLOYSITE NANOTUBES FOR ENHANCED REMOVAL OF Hg^{2+} IONS FROM AQUEOUS SOLUTIONS

Salvatore Cataldo[1], Francesco Crea[2], Marina Massaro[3], Demetrio Milea[2], Alberto Pettignano[1,*], and Serena Riela[3]

[1] Dipartimento di Fisica e Chimica – Emilio Segrè, Università di Palermo, Viale delle Scienze, 90128 Palermo, Italy
[2] Dipartimento Di Scienze Chimiche, Biologiche, Farmaceutiche Ed Ambientali, Università degli Studi di Messina, Viale F. Stagno d'Alcontres, 31, 98166 Messina, Italy
[3] Dipartimento di Scienze e Tecnologie Biologiche, Chimiche e Farmaceutiche, Università di Palermo, Viale delle Scienze, 90128 Palermo, Italy

Abstract—Water is essential for humans, animals, and plants; pollutants, usually derived from anthropogenic activities, can have a serious effect on its quality. Heavy metals are significant pollutants and are often highly toxic to living organisms, even at very low concentrations. Among the numerous removal techniques proposed, adsorption onto suitable adsorbent materials is considered to be one of the most promising. The objective of the current study was to determine the effectiveness of halloysite nanotubes (HNT) functionalized with organic amino or thiol groups as adsorbent materials to decontaminate polluted waters, using the removal of Hg^{2+} ions, one of the most dangerous heavy metals, as the test case. The effects of pH, ionic strength (I), and temperature of the metal ion solution on the adsorption ability and affinity of both materials were evaluated. To this end, adsorption experiments were carried out with no ionic medium and in $NaNO_3$ and NaCl at $I = 0.1$ mol L^{-1}, in the pH range 3–5 and in the temperature range 283.15–313.15 K. Kinetic and thermodynamic aspects of adsorption were considered by measuring the metal ion concentrations in aqueous solution. Various equations were used to fit experimental data, and the results obtained were explained on the basis of both the adsorbent's characterization and the Hg^{2+} speciation under the given experimental conditions. Thiol and amino groups enhanced the adsorption capability of halloysite for Hg^{2+} ions in the pH range 3–5. The pH, the ionic medium, and the ionic strength of aqueous solution all play an important role in the adsorption process. A physical adsorption mechanism enhanced by ion exchange is proposed for both functionalized materials.

Keywords—Adsorption · Halloysite · Mercury · Remediation · Speciation

INTRODUCTION

Among toxic metals, Hg is considered to be one of the most dangerous to humans and all other living organisms as shown by the results of numerous toxicological studies (e.g. Bernhoft 2012; Ynalvez et al. 2016). For this reason, many research programs exist which are devoted to the monitoring and assessment of Hg diffusion in the environment, supported by national and international organizations (UN Environment 2019). Three types of Hg sources are responsible for environmental contamination, namely, natural, anthropogenic, and a third source related to the remobilization of previously settled Hg from soils and sediments (Wang et al. 2004). Based on a rough estimate, 30% of Hg emissions in the atmosphere are of anthropogenic origin and the amount of anthropogenic Hg released into natural waters is ~1000 tons per year (UN Environment 2019). Due to biogeochemical transformations, Hg in natural waters can be present in elemental (Hg^0), inorganic (Hg^+, Hg^{2+}), or organic [CH_3Hg^+, $(CH_3)_2Hg$] forms. All species of Hg react with other components of aquatic systems to complicate its speciation picture (Von Burg and Greenwood 1991). Among the various forms, methylmercury is considered to be the most toxic whilst the inorganic species, especially Hg^{2+}, are the most soluble and abundant in polluted waters (Wang et al. 2004)

Considering the persistence of the element in the environment, the only solution to the 'mercury problem' is the reduction of anthropogenic emission. Much work is being done to find a good remediation method for removal of Hg from wastewaters before its release into the environment. One of the most promising techniques for removing toxic metal ions from contaminated aqueous systems is adsorption onto materials of natural origin that are cheap, abundant, and non-toxic (Cataldo et al. 2016, 2018; De Gisi et al. 2016). Among natural adsorbent materials, the unique features of clay minerals have attracted great interest. They are cheap, available in large quantities, have little or no toxicity of their own, and have a very small environmental impact (Dong et al. 2012; Cataldo et al. 2015). Several types of clay minerals have already been used as adsorbents of pollutants, natural or modified, in remediation studies and, among them, halloysite is one of the most interesting (Dong et al. 2012; Cataldo et al. 2015; 2018; Peng et al. 2015; Renu et al. 2017; Uddin 2017).

Halloysite is a clay mineral with a mainly hollow tubular structure which consists of 10–15 aluminosilicate layers

* E-mail address of corresponding author: alberto.pettignano@unipa.it
DOI: 10.1007/s42860-021-00112-1

with outer and inner surfaces consisting of siloxane, silanol, and aluminol groups (Joussien et al. 2005). Due to this particular structure, HNT are positively charged inside and negatively charged outside over a wide pH range (Bretti et al. 2016). The charge separation and the tubular structure enable this clay mineral to be used in many applications, e.g. as a drug carrier and in drug delivery, as a catalyst support, as a filler for hydrogels and polymers, as an adsorbent of pollutants, etc. (Abdullayev et al. 2010; Dong et al. 2012; Kamble et al. 2012; Wei et al. 2013; Owoseni et al. 2014; Cataldo et al. 2018; Massaro et al. 2020).

In a recent study, a commercial halloysite and its functionalized form with amino groups were used to good effect as adsorbents of Pb^{2+} ions (Cataldo et al. 2018). In the present study, the objective was to test the same pristine halloysite (p-Hly) and two functionalized forms with amino groups (Hly-NH_2) and thiol groups (Hly-SH) as adsorbents for the removal of Hg^{2+} ions from aqueous solutions, with the hypothesis, as proven in various previous studies (e.g. Cataldo et al. 2013, 2018), that the adsorption capacity of a material depends not only on its affinity toward the pollutant, but also on the experimental conditions (pH, ionic medium, ionic strength, temperature) of the aqueous solution containing the pollutant to be removed and that this aspect is even more important when the pollutant is a metal ion such as Hg^{2+}.

The Hg^{2+} ion forms quite stable hydrolytic and chloride species in the pH range typical of natural waters and industrial wastewaters and with the anion commonly present in these water matrices (Baes and Mesmer 1976; Martell and Smith 1977; Martell et al. 2004; Crea et al. 2014). With this in mind, adsorption experiments were carried out for both functionalized clay materials, adjusting the experimental conditions of the solutions containing Hg^{2+} ions. The results together with the characterization of the clay materials (Cataldo et al. 2018; Massaro et al. 2019) were analyzed in order to: (1) establish the effect of halloysite functionalization, the kinetics and thermodynamics of Hg^{2+} ion adsorption, and the best experimental conditions in terms of adsorption ability of both materials; and (2) evaluate the mechanism of adsorption.

MATERIALS AND METHODS

Chemicals and Materials

Pristine halloysite (p-Hly) was a commercial product (Sigma, lot MKBQ8631V) and was used after washing with ultrapure water ($\rho \geq 18$ MΩ cm) and drying in an oven at $T = 383.15$ K. 3-azido propyltrimethoxisilane was synthesized as reported elsewhere (Massaro et al. 2016); 3-mercapto propyltrimethoxysilane and all reagents needed for the synthesis were purchased from Sigma-Aldrich (Steinheim, Germany) and used without further purification.

Sodium nitrate and sodium chloride pure salts (Fluka) were used, after drying at 383.15 K for 2 h, to adjust the ionic strength of solutions. Nitric acids and sodium hydroxide used to adjust the pH of the metal ion solutions were prepared by diluting concentrated Fluka solutions. Hg^{2+} ion solutions were prepared by weighing the $Hg(NO_3)_2$ (Sigma-Aldrich, Steinheim, Germany), analytical grade salt. Mercury standard solutions used for calibration curves were prepared by diluting a 1000 mg L^{-1} standard solution in 2% HNO_3 (CertiPUR, Merck, Darmstadt, Germany). All the solutions were prepared using fresh, CO_2-free, ultrapure water ($\rho \geq 18$ MΩ cm) and grade A glassware.

Synthesis of Hly-NH_2 and Hly-SH Nanomaterials

The adsorbent materials were obtained following procedures reported previously (Cataldo et al. 2018; Massaro et al. 2019). In particular, the pristine halloysite was reacted with the appropriate silane (3-mercaptopropyltrimethoxysilane or 3-azidopropyltrimethoxysilane, respectively) to give the compounds Hly-SH and Hly-N_3 (Fig. 1).

The latter was then subjected to reduction under the Staudinger reaction conditions (triphenylphosphine, DMF, r.t.), to obtain, finally, the Hly-NH_2 material with significant organic moiety loading. The degrees of functionalization of halloysite, estimated using thermogravimetric analysis, were 0.40 mmol g^{-1} and 0.07 mmol g^{-1} for Hly-SH and Hly-NH_2, respectively. The successful functionalization was also verified by Fourier-transform infrared (FTIR) spectroscopy (Fig. 2).

The FTIR spectrum of the thiol-functionalized Hly (Fig. 2c) showed the typical Hly vibration stretching bands, (Massaro et al. 2016) and, in addition, exhibited the vibration bands for C–H stretching of methylene groups around 2980 cm^{-1} attributed to the organic functionalities introduced. In the FTIR spectrum of Hly-NH_2 (Fig. 2a), in addition to the aforementioned vibration stretching bands, a strong vibration band at ~1500 cm^{-1} due to the bending vibrations of the -NH_2 groups was also present (Cataldo et al. 2018; Massaro et al. 2018).

The concentrations of the silanol and aluminol groups in p-Hly ($C_{SiOH} = 0.80$ mmol g^{-1}; $C_{AlOH} = 0.20$ mmol g^{-1}) were calculated, in a previous study, by direct potentiometric titrations (Bretti et al. 2016). Considering that each amino or thiol group substitutes a silanol group of p-Hly, the SiOH:AlOH:SH and SiOH:AlOH:NH_2 ratios were 0.40:0.20:0.40 mmol g^{-1} and 0.73:0.20:0.07 mmol g^{-1}, respectively.

Experimental Equipment and Procedures for Kinetic and Thermodynamic Experiments

Batch experiments were carried out in order to study the kinetic and thermodynamic aspects of Hg^{2+} adsorption onto p-Hly, Hly-NH_2, and Hly-SH.

In kinetic experiments, ~15 mg of adsorbent material was placed in 12 Erlenmeyer flasks containing 25 mL of $Hg(NO_3)_2$ solution ($c_{Hg^{2+}} \approx 40$ mg L^{-1}), at pH = 4, with no added ionic medium, and at $T = 298.15$ K. The Hg^{2+} ion concentration in solution was measured at various adsorbent–solution contact times over the time interval 0–360 min. The pH of solution was monitored during the experiments.

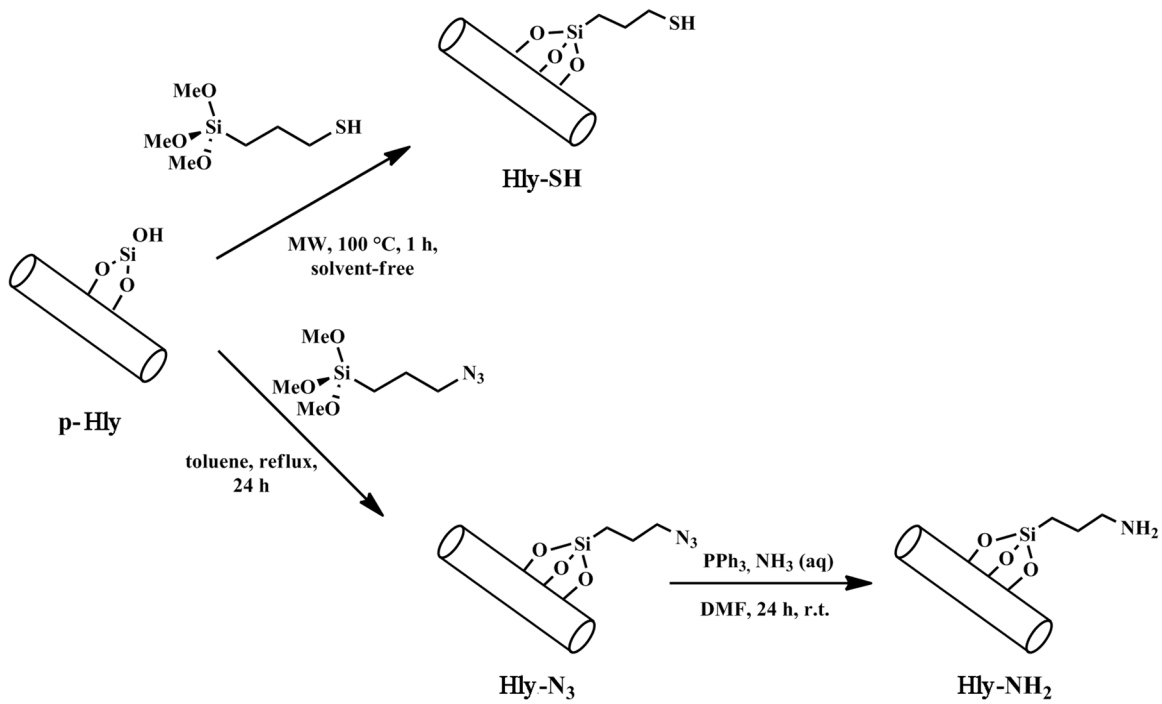

Fig. 1 Schematic representation of Hly-NH_2 and Hly-SH synthesis

Isotherm experiments were carried out in the pH range 3–5, with no ionic medium, in 0.1 mol L^{-1} $NaNO_3$, in NaCl (with Hly-SH adsorbent only), and over the temperature range 283.15–313.15 K. In each equilibrium experiment, ~15 mg of adsorbent material was placed in nine Erlenmeyer flasks containing 25 mL of $Hg(NO_3)_2$ solution at various concentrations ($5 \leq c_{Hg^{2+}}$ (mg L^{-1}) ≤ 50). The solutions were stirred at 180 rpm for 12 h using an orbital mixer (model M201-OR, MPM Instruments, Bernareggio, Italy) and then were separated from the adsorbent before measuring the pH and the Hg^{2+} concentration.

The concentrations of Hg^{2+} ions in the solutions collected in kinetic and isotherm experiments were measured by Inductively Coupled Plasma Optical Emission Spectroscopy

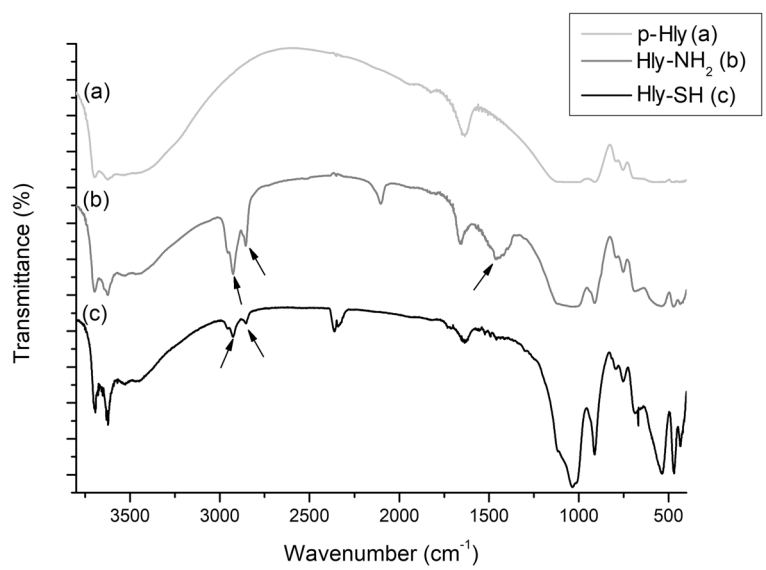

Fig. 2 FTIR spectra of p-Hly, Hly-NH_2, and Hly-SH

(ICP-OES) using a Perkin Elmer (Waltham, USA) Model Optima 2100 instrument, equipped with an autosampler model AS-90. The Hg emission intensity was measured and each measurement was repeated three times. Calibration curves were measured in the same experimental conditions and covering the Hg^{2+} ion concentration range of kinetic and thermodynamic adsorption experiments. The pH of the Hg^{2+} ion solutions was measured with a combined ISE-H^+ glass electrode (Ross type 8102, Thermoscientific, Waltham, USA). The ISE-H^+ electrode was calibrated previously under the same experimental conditions as the adsorption experiments. To this end, 25 mL of standardized HNO_3 solution was titrated with NaOH using a potentiometric titration system (Metrohm, Herisau, Switzerland, Model 888 Titrando) controlled by the *TIAMO* software (version 2.3 light, Metrohm - Herisau, Switzerland).

Kinetic and Isotherm Models for Hg^{2+} Ion-adsorption Studies

Kinetic data were fitted with the pseudo-first order equation (PFO) of Lagergren (Eq. 1), the pseudo-second order equation (PSO) (Eq. 2), and the intraparticle diffusion equation of Vermeulen (Ver) (Eq. 3) (Lagergren 1898; Blanchard et al. 1984; Guo et al. 2008):

$$\frac{dq_t}{dt} = \mathrm{k}_1(q_e - q_t) \tag{1}$$

$$\frac{dq_t}{dt} = \mathrm{k}_2(q_e - q_t)^2 \tag{2}$$

$$\frac{dq_t}{dt} = \mathrm{k}_\mathrm{v}\frac{(q_e^2 - q_t^2)}{q_t} \tag{3}$$

where q_t and q_e represent the adsorption capacity of the p-Hly, Hly-NH_2, or Hly-SH (mg g^{-1}) at time t and at equilibrium and k_1 (min^{-1}), k_2 (g mg^{-1} min^{-1}), and k_v (min^{-1}) are the rate constants of adsorption. In the present study, the integrated forms of equations for the boundary conditions $t=0$ to $t=t$ and $q_t=0$ and $q_t=q_t$, listed below, were used:

$$q_t = q_e(1 - e^{-\mathrm{k}_1 t}) \tag{4}$$

$$q_t = \frac{q_e^2 \mathrm{k}_2 t}{1 + q_e \mathrm{k}_2 t} \tag{5}$$

$$q_t = q_e(1 - e^{-2\mathrm{k}t})^{0.5} \tag{6}$$

The adsorption equilibrium data were processed with Freundlich (F) (Eq. 7) and Langmuir (L) (Eq. 8) isotherm equations (Freundlich 1906; Langmuir 1918):

$$q_e = \mathrm{K_F} c_e^{1/n} \tag{7}$$

$$q_e = \frac{q_m \mathrm{K_L} c_e}{1 + \mathrm{K_L} c_e} \tag{8}$$

where q_m (mg g^{-1}) is the maximum adsorption ability of the adsorbent, c_e (mg L^{-1}) is the Hg^{2+} concentration in solution at equilibrium; K_F ($L^{1/n}$ g^{-1} $mg^{1-1/n}$) and K_L (L·mg^{-1}) are the constants in the Freundlich and Langmuir models, respectively.

The Hg^{2+} ion-adsorption capacity at various contact times t (q_t, mg g^{-1}) in kinetic experiments, or at different Hg^{2+}/adsorbent ratios in the thermodynamic studies (q_e, mg g^{-1}) were calculated using Eq. 9:

$$q_t \text{ or } q_e = \frac{V(c_0 - c_t)}{m} \tag{9}$$

where V (L) is the volume of the Hg^{2+} solution and m is the mass (g) of the adsorbent material (p-Hly, Hly-NH_2, or Hly-SH); c_0 and c_t are the Hg^{2+} ion concentrations (mg L^{-1}) at $t=0$ and $t=t$, respectively. At equilibrium conditions, Eq. 9 was used by replacing c_t with c_e to calculate q_e.

The conditional Langmuir constant values (in 0.1 mol L^{-1} $NaNO_3$, pH=3.5; $c_{Hg}{}^{2+}$ in mol L^{-1}) (Liu 2009) in the temperature range 283.15–313.15 K were used to calculate the thermodynamic state functions ΔG (kJ mol^{-1}), ΔH (kJ mol^{-1}), and ΔS (kJ mol^{-1} K^{-1}) by using the Gibbs and van't Hoff equations (Eqs. 10, 11). The following assumptions were made: (1) the adsorption was reversible; (2) the stoichiometry of adsorption did not change; and (3) equilibrium was established during the adsorption experiments (Crini and Badot 2008; Tran et al. 2016).

$$\Delta G = -\mathrm{R}T\ln\mathrm{K_L} \tag{10}$$

$$\ln\mathrm{K_L} = -\frac{\Delta H}{\mathrm{R}T} + \frac{\Delta S}{R} \tag{11}$$

where R is the universal gas constant, 0.008314 kJ mol^{-1} K^{-1}, and T is the temperature in K.

The *LIANA* and *OriginLab* suite software (OriginLab Corporation, Northampton, Massachusetts, USA), were used to fit kinetic and isotherm equations to experimental data.

RESULTS AND DISCUSSION

Speciation Analysis

The percentage of protonated/unprotonated functional groups of the adsorbent material, the charge of the species formed by the metal ions, and the experimental conditions (ionic medium, ionic strength, pH) for the aqueous solutions to be treated all play an important role in the efficiency of metal-ion sorption. Opposite charges for the metal ion species and for the surface of adsorbent material undoubtedly favor the adsorption process via Coulombic attraction. For this reason, knowledge of the species distribution of both metal ions and adsorbent material is required in order to discuss the adsorption results effectively.

According to previously reported studies on the acid-base properties of the pristine material, aluminol groups are fully protonated in the pH range investigated in this work, while the silanols are partially deprotonated: 50% of Si–OH groups are protonated at pH = log $K^H \approx 4$, with increasing fraction of protonated and deprotonated groups below and above this pH value, respectively (Bretti et al. 2016).

Other experiments need to be performed using pure water (no ionic medium added) and solutions containing Na^+ salts as the ionic medium (i.e. $NaNO_3$ and NaCl at $I = 0.1$ mol L^{-1}). In fact, as already reported, Na^+ ions form weak ion pairs with silanol groups (Bretti et al. 2016). Despite their weakness, relatively large Na^+ ion concentrations (relative to that of the sorbent material) led to formation percentages of sodium ion pairs that are not negligible and, interestingly, modify the charge of material surface and reduce the number of available binding sites (occupied by sodium itself).

For the materials functionalized with -NH_2 or -SH groups, though the protonation constants have not been determined experimentally, both amino and thiol functions can be assumed to be fully protonated in the above-mentioned pH range (3–5), as aliphatic amines and thiols generally show log $K^H >> 6$ (e.g. log $K^H \approx 10.6$ and 10.9 for propylamine and propane 2-thiol, respectively (Martell et al. 1977, 2004)). Of course, complexation by metal cations may result in proton displacement from the protonated functional groups. The soft nature of S donors should facilitate H^+ exchange by Hg^{2+}, although -NH_2 groups also have good affinity toward these cations. In fact, from a rough estimate of the contribution of the S- and N- donors to the $\log K_{HgL}$ of a generic ligand L, based on the stability constant values of 143 amines and 92 thiols, on average, the contribution of -SH and -NH_2 groups to the stability of the HgL species has been shown to be 22.3 and 6.4 log units, respectively (Crea et al. 2014).

Another important aspect to take into account in evaluating the results obtained here is the speciation of Hg^{2+} ions, which are subjected to a strong ionic medium effect due to the ability of Hg to form stable chloride complexes (Crea et al. 2014). In pure water or low-interacting media (e.g. $NaNO_3$, see speciation diagram in Supplementary Material Fig. S1a), Hg is present as free cations and/or in its hydrolyzed forms ($Hg(OH)^+$ and $Hg(OH)_2$), in percentages which depend on pH. Hydrolysis is suppressed completely at pH < 6.0 in NaCl media, in which $HgCl_r^{(2-r)}$ (with $1 \le r \le 4$) complexes dominate Hg speciation, with ratios between these species depending on Cl^- concentration (e.g. in NaCl at $I = 0.1$ mol L^{-1}, the percentages of chloride species are: $HgCl_2 \approx 38\%$, $HgCl_3^- \approx 44\%$, $HgCl_4^{2-} \approx 18\%$) (see speciation diagram in Fig. S1b) (Baes and Mesmer 1976; Crea et al. 2014).

Kinetics of Adsorption of Hg^{2+} Ions onto Hly-NH_2 and Hly-SH Materials

The kinetics of the adsorption of Hg^{2+} ions onto the two functionalized halloysite materials were studied in solution with no ionic medium, at initial pH = 4. The kinetic data have been fitted with PFO, PSO, and Ver kinetic models.

The kinetic constants and q_e values are reported in Table 1 together with the experimental q_e (measured after 24 h), and the corresponding R^2 and standard deviation values of the fits. From comparison of statistical parameter values, although all the models gave a quite good fit, the Ver and the PFO can be considered the best models (the largest R^2 and the smallest standard deviation values of the fits) for Hg^{2+} adsorption onto Hly-SH and Hly-NH_2 adsorbents, respectively. The goodness of model fits were confirmed by comparisons between the experimental and calculated q_e values. The experimental data together with the fitted curves of the three kinetic equations are reported in Fig. 3 for both of the Hg^{2+}-adsorbent systems.

Table 1 Parameters of PFO, PSO, and Ver kinetic equations for Hg^{2+} ion adsorption on Hly-NH_2 and Hly-SH, at pH = 4, without the addition of ionic medium and at $T = 298.15$ K

Kinetic model	Adsorbent	$q_{e\,exp}$ [a]	$q_{e\,calc}$ [b]	k_i [c,d]	R^2	σ [e]
PFO			22.2 ± 0.6	0.095 ± 0.009	0.9713	1.3581
PSO	Hly-SH	22.6	23.4 ± 0.4	0.0058 ± 0.0001	0.9835	1.0298
Ver			22.7 ± 0.4	0.020 ± 0.002	0.9883	0.8667
PFO			16.2 ± 0.3	0.065 ± 0.004	0.9904	0.6211
PSO	Hly-NH_2	16.2	17.4 ± 0.4	0.0052 ± 0.0001	0.9856	0.7595
Ver			16.5 ± 0.4	0.014 ± 0.002	0.9777	0.9449

[a] mean value of experimental data at equilibrium

[b] mg g^{-1}, ± std. dev.

[c] min^{-1} for both k_1 and k_v, g mg^{-1} min^{-1} for k_2, ± std. dev.

[d] subscript *i* is 1, 2, or v according to the model

[e] std. dev. of the fit

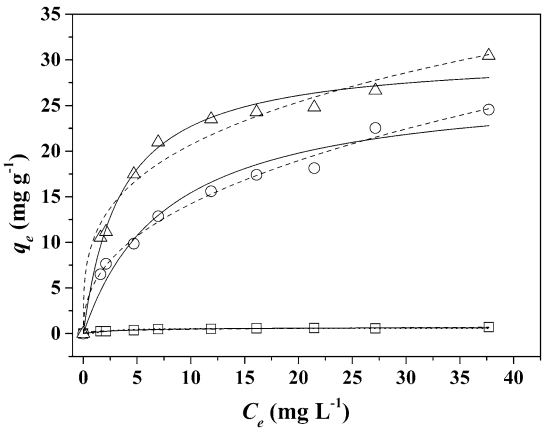

Fig. 3 Dependence of q_t (mg g^{-1}) on contact time for Hg^{2+} ion adsorption onto Hly-NH_2 (□) and Hly-SH (○) adsorbents. Data are fitted with PFO (dashed line), PSO (continuous line), and Ver (dotted line) kinetic equations. Experimental conditions: 15 mg of adsorbent material; $I \rightarrow 0$ mol L^{-1}; $Hg(NO_3)_2$ ($c_{Hg}{}^{2+} = 40$ mg L^{-1}), pH = 4, $T = 298.15$ K

Differences in adsorption kinetics of the two adsorbents can be attributed to their different degrees of functionalization (see the sections above on 'Synthesis of Hly-NH_2' and 'Hyl-SH Nanomaterials'). Because the thiols are soft ligands, they have a greater affinity for the metal ion as confirmed by the greater q_e values. For both of the adsorbent materials, adsorption equilibrium is reached after~200 min. The results obtained with Hly-SH agree with those found by Manohar et al. (2002) for the Hg^{2+} ion adsorption onto a clay (Thonnakkal Clay Mine;>90% kaolinite and mica) functionalized with thiol groups with 2-mercaptobenzimidazole. The current authors found a q_e of 23.839 mg g^{-1} and a k_2 of 2.011 10^{-3} g mg^{-1} min^{-1} at pH=6, $T = 30$°C, and $c_{Hg2+} = 50$ mg L^{-1}.

Modeling the Equilibrium Adsorption of Hg^{2+} Ions by Pristine and Functionalized Hly Materials

Batch adsorption experiments were done to establish the adsorption capabilities, the adsorption affinities, and the adsorption mechanisms of p-Hly and of the two functionalized halloysites for Hg^{2+} ions. Langmuir and Freundlich equations (all equations are two-parameter models) were used to fit the experimental data at various experimental conditions. The adsorption experiments were carried out over a limited pH range (3–5) in order to minimize the effect of Hg^{2+} hydrolysis (see the section above on Speciation Analysis). The background salt and temperature effects were evaluated using 0.1 mol L^{-1} $NaNO_3$ or NaCl as ionic media and varying the temperature in the range 283.15–313.15 K. The parameters of the two models are reported in Tables 2 and 3 together with statistical parameters of fits.

Table 2 Freundlich (F) and Langmuir (L) isotherm parameters for Hg^{2+} ion adsorption on p-Hly, Hly-SH, and Hly-NH_2 in the pH range 3–5, with no ionic medium ($I \rightarrow 0$ mol L^{-1}) and at $T = 298.15$ K

Material	Model	pH[a]	q_m[b]	K_x[c]	n	R^2	σ[d]
	L	3.0	0.71 ± 0.03	0.27 ± 0.04		0.9710	0.0363
	F	3.0		0.23 ± 0.02	3.3 ± 0.3	0.9673	0.0386
	L	4.0	4.5 ± 0.1	0.11 ± 0.01		0.9962	0.0751
p-Hly	F	4.0		0.67 ± 0.07	2.0 ± 0.1	0.9782	0.1792
	L	5.0	4.2 ± 0.9	0.05 ± 0.02		0.9633	0.1554
	F	5.0		0.28 ± 0.08	1.5 ± 0.2	0.9397	0.1991
	L	3.0	30.7 ± 0.9	0.29 ± 0.03		0.9845	1.1542
	F	3.0		10.5 ± 0.8	3.4 ± 0.3	0.9732	1.5147
Hly-SH	L	4.0	30.5 ± 0.8	0.27 ± 0.02		0.9928	0.7951
	F	4.0		8.8 ± 0.7	2.8 ± 0.2	0.9777	1.3977
	L	5.0	26 ± 1	0.29 ± 0.04		0.9843	0.9656
	F	5.0		8 ± 1	2.7 ± 0.4	0.9183	2.2027
	L	3.0	27 ± 2	0.13 ± 0.03		0.9621	1.4853
	F	3.0		5.5 ± 0.3	2.4 ± 0.1	0.9918	0.6914
	L	4.0	30 ± 1	0.11 ± 0.01		0.9941	0.6218
Hly-NH_2	F	4.0		4.4 ± 0.3	2.0 ± 0.1	0.9888	0.8544
	L	5.0	20.2 ± 0.7	0.20 ± 0.02		0.9916	0.5263
	F	5.0		4.5 ± 0.5	2.3 ± 0.3	0.9475	1.3136

[a] initial pH of metal ion solutions

[b] parameter values in mg g^{-1} ± std. dev.

[c] x = L or F, constant values in L$^{1/n}$ g^{-1} mg$^{1-1/n}$ for K_F, L mg^{-1} for K_L ± std. dev.

[d] std. dev. of the fit

Table 3 Freundlich (F) and Langmuir (L) isotherm parameters for Hg^{2+} ion adsorption on Hly-SH and Hly-NH_2 at pH = 3.5, in $NaNO_3$, at I = 0.1 mol L^{-1}, and in the temperature range 283.15–313.15 K

Adsorbent	Model	T^a	$q_m{}^b$	$K_x{}^c$	n	R^2	σ^d
Hly-SH	L	283.15	18.3 ± 0.4	1.3 ± 0.1		0.9947	0.3949
Hly-SH	F	283.15		10.0 ± 0.5	3.3 ± 0.5	0.9458	1.2692
Hly-SH	L	298.15	19.3 ± 0.6	2.5 ± 0.3		0.9918	0.5364
Hly-SH	F	298.15		12.3 ± 0.4	3.0 ± 0.4	0.9762	0.9136
Hly-SH	L [e]	298.15	46 ± 2	2.4 ± 0.5		0.9580	3.1691
Hly-SH	F [e]	298.15		32 ± 2	9 ± 2	0.9367	3.8898
Hly-SH	L	313.15	18.2 ± 0.9	4.1 ± 0.8		0.9640	1.1359
Hly-SH	F	313.15		13.1 ± 0.8	4.1 ± 0.9	0.8822	2.0548
Hly-NH_2	L	283.15	9.8 ± 0.6	1.0 ± 0.2		0.9720	0.5104
Hly-NH_2	F	283.15		5.1 ± 0.3	3.5 ± 0.6	0.9692	0.5359
Hly-NH_2	L	298.15	9.7 ± 0.5	1.5 ± 0.3		0.9764	0.4784
Hly-NH_2	F	298.15		5.8 ± 0.4	4.2 ± 0.8	0.9621	0.6068
Hly-NH_2	L	313.15	8.6 ± 0.2	2.0 ± 0.3		0.9897	0.2812
Hly-NH_2	F	313.15		5.8 ± 0.2	5.6 ± 0.9	0.9763	0.4258

[a] Kelvin

[b] parameter values in mg g^{-1} ± std. dev.

[c] x = L or F, constant values in $L^{1/n}$ g^{-1} $mg^{1-1/n}$ for K_F, L mg^{-1} for K_L ± std. dev.

[d] std. dev. of the fit

[e] in 0.1 mol L^{-1} NaCl

The experimental data, together with the fitted curves of the two isotherm models, are reported in Fig. 4 and in Figs S2–S7. The largest R^2 and smallest standard deviations of the fits were obtained using the Langmuir model. For this reason, the sorption abilities and affinities of both the adsorbent materials for Hg^{2+} were analyzed using the parameters obtained using the Langmuir equation.

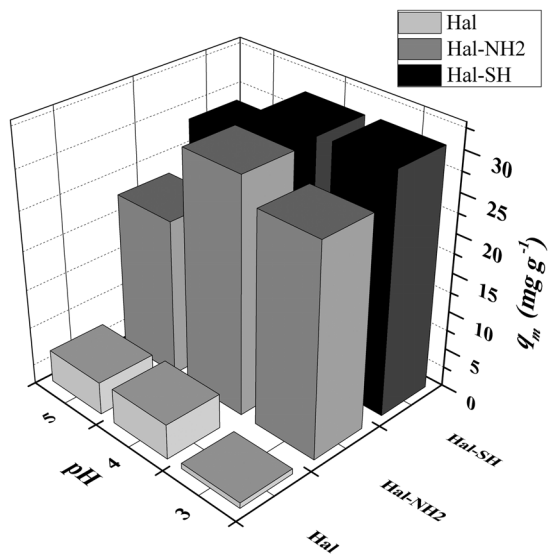

Fig. 4 Adsorption isotherms of Hg^{2+} ions on p-Hal (□), Hly-SH (Δ), and Hly-NH_2 (○) from aqueous solutions at pH = 3, with no ionic medium and at T = 298.15 K. Experimental data fitted with Freundlich (dashed lines) and Langmuir (continuous lines) isotherm equations

Although the Langmuir model, as well as the other isotherm equation, is an empirical model, the best fit of which does not necessarily mean a specific adsorption mechanism, the adsorption of Hg^{2+} ions onto Hly-NH_2 and Hly-SH is a monolayer adsorption due to the presence of the two functional groups grafted onto the external surface of p-Hly (-NH_2 or -SH). Indeed, at the same pH, the adsorption ability of p-Hly is almost zero or, in any case, very small compared to that of functionalized Hly (see Table 2). Moreover, each Hg^{2+} ion occupies, hypothetically, a site which is no more available for the other metal ions in aqueous solution.

In general, the functionalization of p-Hly with thiol or amino groups increased its adsorption ability toward Hg^{2+} ions in the pH range investigated (e.g. at pH = 4, q_m = 4.5, 30.5, and 30 mg g^{-1} for p-Hly, Hly-SH, and Hly-NH_2, respectively) (Table 2, Fig. S2). The experimental conditions for the metal ion solution (pH, ionic medium, and temperature) play an important role in the adsorption process and are summarized as follows:

(1) the adsorption capabilities of Hly-NH_2 and Hly-SH at initial pH 3 and 4, and $I \rightarrow 0$ mol L^{-1} are almost the same and in both systems (Hg^{2+} ions adsorbent) decrease at pH = 5 with the most pronounced decrease being for Hly-NH_2 material (Table 2, Fig. 5);
(2) the addition of 0.1 mol L^{-1} $NaNO_3$ to the Hg^{2+} solution caused a decrease in adsorption capability for both functionalized halloysites (Table 3, Fig. 6, and Figs S4, S5, and S7);

(3) the addition of 0.1 mol L^{-1} NaCl to the Hg^{2+} solution, done only in the experiments with Hly-SH material, increased its adsorption ability (Table 3, Fig. 6, and Fig. S6);
(4) independent of the experimental conditions, the affinity (K_L) of Hly-SH for Hg^{2+} ion was greater than that of Hly-NH_2;
(5) the affinity (K_L) of both Hly-NH_2 and Hly-SH materials for Hg^{2+} ion increased with increasing temperature of the metal ion solution (e.g. for Hly-SH, at pH = 3.5 and in 0.1 mol L^{-1} $NaNO_3$, K_L = 1.3, 2.5, and 4.1 L mg^{-1} at T = 283.15, 298.15, and 313.15 K, respectively). Changing temperature caused no significant changes in q_m (Table 3).

The greater affinity and adsorption ability of Hly-SH relative to Hyl-NH_2 was attributed to the greater degree of functionalization (0.4 mmol g^{-1} and 0.07 mmol g^{-1} for Hly-SH and HlY-NH_2, respectively) together with the greater affinity of thiol groups for Hg^{2+} ions due to the soft nature of S-donor ligands.

Considering that, at the pH investigated, the amino groups and thiol groups were fully protonated (see the section on Speciation Analysis above), an ionic exchange may, conceivably, have occurred during Hg^{2+} adsorption on both functionalized adsorbent materials. Although the H^+ displacement should be favored by the soft nature of SH groups, at pH $\leq$ 4, the high H^+ concentration caused a flattening of the differences in adsorption capability of Hly-SH and Hly-NH_2, reducing the binding of Hg^{2+} ions.

The reduction in adsorption capability of both functionalized halloysites in 0.1 mol L^{-1} $NaNO_3$ was justified by assuming, as mentioned above, the competition of sodium cations, which are much more concentrated than

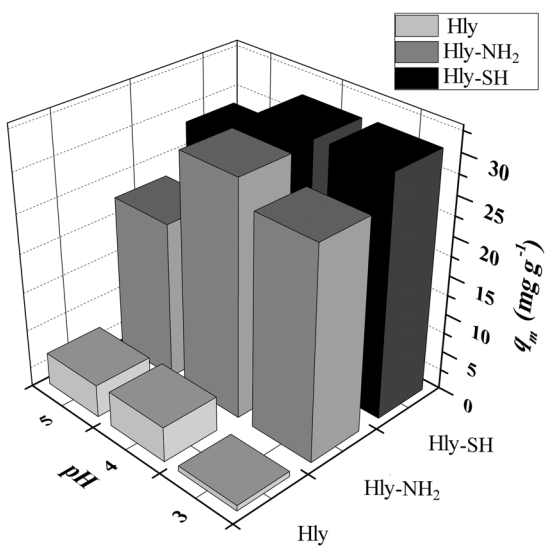

Fig. 5 q_m values of Hg^{2+} ion adsorption onto p-Hly, Hly-SH, and Hly-NH_2 from aqueous solutions at various pH values, with no ionic medium and at T = 298.15 K

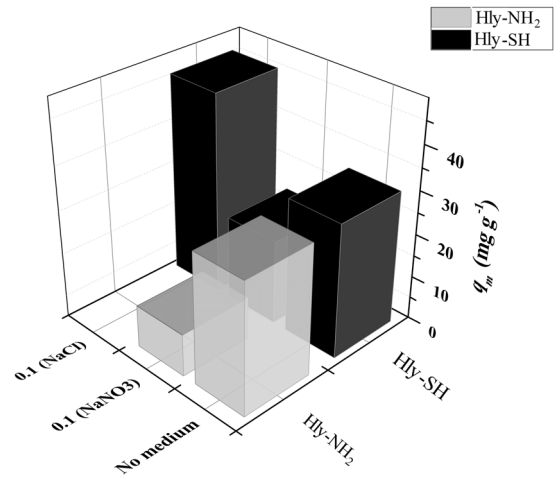

Fig. 6 q_m values of Hg^{2+} ion adsorption onto Hly-SH and Hly-NH_2 from aqueous solutions at pH = 3.5/4, in 0.1 mol L^{-1} $NaNO_3$, 0.1 mol L^{-1} NaCl, and with no ionic medium, at T = 298.15 K

Hg^{2+} ions. Nevertheless, when the anion of background salt is chloride, at the same ionic strength, an improvement of the adsorption capacity of Hly-SH was found (q_m = 30.5, 19.3, 46 mg g^{-1} at $I \rightarrow 0$ and at I = 0.1 mol L^{-1} in $NaNO_3$ and NaCl medium, respectively). The same adsorption improvement with increasing NaCl concentration ($0 \leq I$ (mol L^{-1}) ≤ 0.1) was found by Manohar et al. (2002) for Hg^{2+} adsorption onto a natural clay impregnated with 2-mercaptobenzimidazole. The formation of Hg^{2+}-Cl^- species probably changed the speciation picture of the metal ion, increasing the percentages of neutral and negatively charged Hg species ($HgCl_2$, $HgCl_3^-$, $HgCl_4^{2-}$) in solution. In support of this hypothesis, Walcarius and Delacôte (2005) found that the adsorption of positively charged species of mercury (Hg^{2+}, $HgOH^+$) onto thiol functionalized mesoporous silicas reduced their adsorption capability. Those authors attributed this reduction to the progressive charging of the adsorbent material which prevented the adsorption of larger amounts of the toxic metal. As a consequence, the adsorption of neutral species avoided the charging of the adsorbent. A further hypothesis related to this adsorption improvement could be the favorable interaction between protonated -SH groups and negatively charged $HgCl_3^-$ and $HgCl_4^-$ species in the pH range investigated.

Considering that, in the pH range investigated, both the -SH and -NH_2 groups of Hly-SH and Hly-NH_2 materials are fully protonated, presumably in proportion to the degree of functionalization, the experimentally observed effect of chloride on the adsorption ability of Hly-SH for Hg^{2+} ions should be the same for Hly-NH_2.

A careful literature search showed that this is the first study dealing with adsorption of Hg^{2+} ions onto functionalized halloysite adsorbents. Some rough comparisons can be made with various clay or silica adsorbent materials

functionalized with the same binding groups. Values for $q_m = 34$ and 118 mg g^{-1} for Hg^{2+} ion adsorption onto sepiolite (SEP) and 3-mercaptopropylsylil-sepiolite (MPS-SEP), at pH = 3, were found by Celis et al. (2000). Considering that MPS-SEP has 0.83 mmol g^{-1} of thiol groups (slightly more than twice that of Hly-SH), the adsorption ability of Hly-SH is comparable ($q_m = 0.71$ and 30.7 mg g^{-1} at pH = 3, for p-Hly and Hly-SH, respectively) and highlights the important role of thiol groups in Hg^{2+} adsorption.

Thermodynamic State Functions of Hg^{2+} Ion Adsorption onto Hly-NH_2 and Hly-SH

The Gibbs and van't Hoff equations were used to calculate the thermodynamic properties ΔG, ΔH, and ΔS. To this end, the conditional values for K_L at pH = 3.5, in $NaNO_3$, at $I = 0.1$ mol L^{-1}, and in the temperature range 283.15–313.15 K were used (Fig. 7). The ΔG, ΔH, and ΔS values (Table 4) revealed that the adsorption of Hg^{2+} ions onto the two functionalized halloysites was a spontaneous process, with negative and very similar ΔG values. Moreover, in both cases, ΔG decreased with increasing temperature from 283.15 to 313.15 K. The adsorption process was endothermic ($\Delta H = 17$ and 28 kJ mol^{-1} for the Hly-NH_2 and Hly-SH adsorbents, respectively) and caused a small positive entropy variation ($\Delta S = 0.16$ and 0.20 kJ mol^{-1} K^{-1} for Hly-NH_2 and Hly-SH adsorbents, respectively). The positive ΔS values, though unremarkable, suggested a structural change in the adsorbent and an increasing randomness at the adsorbent–solution interface (Aksu 2002; Liu and Liu 2008; Tran et al. 2016).

The ΔH values, for both of the adsorbents, at <40 kJ mol^{-1}, are typical of a physical adsorption mechanism (Gereli et al. 2006; Onal et al. 2007; Liu and Liu. 2008; Tran et al. 2016). In the temperature range investigated, the $-\Delta G$ values vary in the ranges 28.7–33.6 and 29.4–35.5 kJ mol^{-1} for Hly-SH and Hly-NH_2 adsorbents, respectively. ΔG values between –20 and 0 kJ mol^{-1} are usually ascribed to a physisorption mechanism, whilst free energy values in the range –20—-80 kJ mol^{-1} are considered typical of adsorption based on ion exchange (Gereli et al. 2006; Onal et al. 2007; Tran et al. 2016). The ΔG values, therefore, suggested a physisorption mechanism probably enhanced by an ion–exchange contribution, in agreement with an hypothesis formed on the basis of acid-base properties of functional groups of adsorbent materials and of the speciation studies of Hg^{2+} ion in aqueous solution.

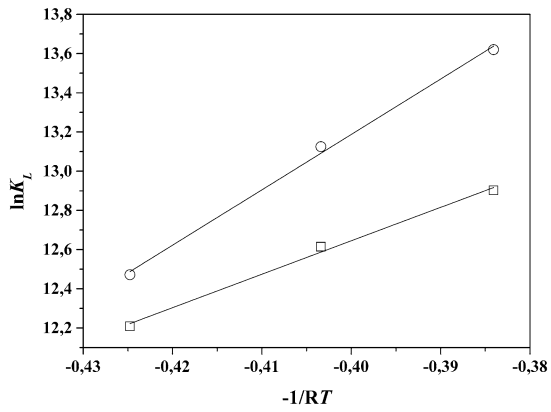

Fig. 7 Plot of $\ln K_L$ vs. $-1/RT$ for the calculation of thermodynamic state functions ΔH and ΔS for Hg^{2+} ion adsorption onto Hly-NH_2 (□) and Hly-SH (○) at pH = 3.5, in 0.1 mol L^{-1} $NaNO_3$ using the van't Hoff equation

Table 4 Thermodynamic state functions ΔG, ΔH, and ΔS for Hg^{2+} ion adsorption onto Hly-NH_2 and Hly-SH from aqueous solution at pH = 3.5, in $NaNO_3$, at $I = 0.1$ mol L^{-1}, in the temperature range 283.15–313.15 K

Adsorbent	T (K)	$-\Delta G^a$	ΔH^a	ΔS^b
Hly-NH_2	283.15	28.7 ± 0.5	17 ± 1	0.16 ± 0.01
Hly-NH_2	298.15	31.3 ± 0.5		
Hly-NH_2	313.15	33.6 ± 0.4		
Hly-SH	283.15	29.4 ± 0.2	28 ± 1	0.20 ± 0.01
Hly-SH	298.15	32.5 ± 0.3		
Hly-SH	313.15	35.5 ± 0.5		

[a] kJ mol^{-1} ± std. dev.

[b] kJ mol^{-1} K^{-1} ± std. dev.

CONCLUSIONS

Halloysites functionalized with amino and thiol groups, previously characterized (Cataldo et al. 2018; Massaro et al. 2019), were used as adsorbent materials for the removal of Hg^{2+} ions from aqueous solutions. The effect of ionic medium, pH, and temperature on the behavior of both adsorbents was evaluated by carrying out kinetic and isotherm experiments under various experimental conditions. The conclusions are summarized as follows:

- Thiol and amino groups increase the adsorption capability of halloysite for Hg^{2+} ions in the pH range 3–5;
- A speciation study of Hg^{2+} ions and of adsorbent materials in aqueous solutions at the same experimental conditions as for adsorption experiments was done. Information about the charge and percentage of Hg^{2+} ions and of adsorbent species in solution were used to interpret the adsorption mechanisms;
- Adsorption equilibria were reached after ~200 min for both Hly-SH and Hyl-NH_2 adsorbents; Ver and the PFO were the best kinetic models for Hg^{2+} adsorption onto Hly-SH and Hly-NH_2 adsorbents, respectively;
- The Langmuir equation gave the best results in terms of isotherm data fit. The maximum adsorption of Hg^{2+} ions by Hly-NH_2 and Hly-SH was obtained in the pH

range 3–4. The addition of 0.1 mol L^{-1} $NaNO_3$ to the Hg^{2+} solution reduced the adsorption capability of both adsorbents. The opposite adsorption behavior was found for 0.1 mol L^{-1} NaCl for Hly-SH;
- Thermodynamic state functions (ΔG, ΔH, and ΔS) of adsorption were calculated from equilibrium adsorption data over the temperature range 283.15–313.15 K;
- The results obtained suggest a physical adsorption mechanism enhanced by the ion-exchange contribution for both functionalized materials.

SUPPLEMENTARY INFORMATION

The online version contains supplementary material available at https://doi.org/10.1007/s42860-021-00112-1.

ACKNOWLEDGMENTS

Funding for Open Access publication has been provided by the Università degli Studi di Palermo as part of the CRUI-CARE Agreement. The authors are grateful to the University of Palermo for financial support.

Funding

Funding sources are as stated in the Acknowledgments.

Declarations

Conflict of Interest

The authors declare that they have no conflict of interest.

REFERENCES

Abdullayev, E., & Lvov, Y. (2010). Clay nanotubes for corrosion inhibitor encapsulation: release control with end stoppers. *Journal of Materials Chemistry, 20,* 6681–6687. https://doi.org/10.1039/C0JM00810A

Aksu, Z. (2002). Determination of the equilibrium, kinetic and thermodynamic parameters of the batch biosorption of nickel(II) ions onto Chlorella vulgaris. *Process Biochemistry, 38,* 89–99. https://doi.org/10.1016/S0032-9592(02)00051-1

Baes, C. F., & Mesmer, R. E. (1976). *The Hydrolysis of Cations*. New York: Wiley

Bernhoft, R.A. (2012). Mercury toxicity and treatment: A review of the literature. *Journal of Environmental and Public Health*, *e460508*, 1–10. https://doi.org/10.1155/2012/460508

Blanchard, G., Maunaye, M., & Martin, G. (1984). Removal of heavy metals from waters by means of natural zeolites. *Water Research, 18,* 1501–1507. https://doi.org/10.1016/0043-1354(84)90124-6

Bretti, C., Cataldo, S., Gianguzza, A., Lando, G., Lazzara, G., Pettignano, A., & Sammartano, S. (2016). Thermodynamics of Proton Binding of Halloysite Nanotubes. *The Journal of Physical Chemistry C, 120,* 7849–7859. https://doi.org/10.1021/acs.jpcc.6b01127

Cataldo, S., Gianguzza, A., Pettignano, A., & Villaescusa, I. (2013). Mercury(II) removal from aqueous solution by sorption onto alginate, pectate and polygalacturonate calcium gel beads. A kinetic and speciation based equilibrium study. *Reactive and Functional Polymers, 73,* 207–217

Cataldo, S., Muratore, N., Orecchio, S., & Pettignano, A. (2015). Enhancement of adsorption ability of calcium alginate gel beads towards Pd(II) ion. A kinetic and equilibrium study on hybrid Laponite and Montmorillonite–alginate gel beads. *Applied Clay Science, 118,* 162–170. https://doi.org/10.1016/j.clay.2015.09.014

Cataldo, S., Gianguzza, A., Milea, D., Muratore, N., & Pettignano, A. (2016). Pb(II) adsorption by a novel activated carbon - alginate composite material. A kinetic and equilibrium study. *International Journal of Biological Macromolecules, 92,* 769–778. https://doi.org/10.1016/j.ijbiomac.2016.07.099

Cataldo, S., Lazzara, G., Massaro, M., Muratore, N., Pettignano, A., & Riela, S. (2018). Functionalized halloysite nanotubes for enhanced removal of lead(II) ions from aqueous solutions. *Applied Clay Science, 156,* 87–95. https://doi.org/10.1016/j.clay.2018.01.028

Celis, R., Hermosin, M. C., & Cornejo, J. (2000). Heavy metal adsorption by functionalized clays. *Environmental Science & Technology, 34,* 4593–4599. https://doi.org/10.1021/es000013c

Crea, F., De Stefano, C., Foti, C., Sammartano, S., & Milea, D. (2014). Chelating agents for the sequestration of mercury(II) and monomethyl mercury(II). *Current Medicinal Chemistry, 21,* 3819–2836. https://doi.org/10.2174/09298673216661406011607 40

Crini, G., & Badot, P.-M. (2008). Application of chitosan, a natural aminopolysaccharide, for dye removal from aqueous solutions by adsorption processes using batch studies: A review of recent literature. *Progress in Polymer Science, 33,* 399–447. https://doi.org/10.1016/j.progpolymsci.2007.11.001

De Gisi, S., Lofrano, G., Grassi, M., & Notarnicola, M. (2016). Characteristics and adsorption capacities of low-cost sorbents for wastewater treatment: A review. *Sustainable Materials and Technologies, 9,* 10–40. https://doi.org/10.1016/j.susmat.2016.06.002

Dong, Y., Liu, Z., & Chen, L. (2012). Removal of Zn(II) from aqueous solution by natural halloysite nanotubes. *Journal of Radioanalytical and Nuclear Chemistry, 292,* 435–443. https://doi.org/10.1007/s10967-011-1425-z

Freundlich, H. M. F. (1906). Over the adsorption in solution. *Journal of Physical Chemistry, 57,* 385–471.

Gereli, G., Seki, Y., Murat Kuşoğlu, İ, & Yurdakoç, K. (2006). Equilibrium and kinetics for the sorption of

promethazine hydrochloride onto K10 montmorillonite. *Journal of Colloid and Interface Science, 299,* 155–162. https://doi.org/10.1016/j.jcis.2006.02.012

Guo, X., Zeng, L., Li, X., & Park, H.-S. (2008). Ammonium and potassium removal for anaerobically digested wastewater using natural clinoptilolite followed by membrane pretreatment. *Journal of Hazardous Materials, 151,* 125–133. https://doi.org/10.1016/j.jhazmat.2007.05.066

Joussein, E., Petit, S., Churchman, J., Theng, B., Righi, D., & Delvaux, B. (2005). Halloysite clay minerals – A review. *Clay Minerals, 40,* 383–426. https://doi.org/10.1180/0009855054040180

Kamble, R., Ghang, M., Gaikawad, S., & Panda, B. (2012). Halloysite nanotubes and applications: A review. *Journal of Advanced Scientific Research, 3,* 25–29.

Lagergren, S. (1898). About the theory of so called adsorption of soluble substances. *Kungliga Svenska Vetenskapsakademiens Handlingar, 24,* 1–39.

Langmuir, I. (1918). The adsorption of gases on plane surfaces of glass, mica and platinum. *Journal of the American Chemical Society, 40,* 1361–1403. https://doi.org/10.1021/ja02242a004

Liu, Y. (2009). Is the free energy change of adsorption correctly calculated? *Journal of Chemical & Engineering Data, 54,* 1981–1985. https://doi.org/10.1021/je800661q

Liu, Y., & Liu, Y.-J. (2008). Biosorption isotherms, kinetics and thermodynamics. *Separation and Purification Technology, 61,* 229–242. https://doi.org/10.1016/j.seppur.2007.10.002

Manohar, D. M., Anoop Krishnan, K., & Anirudhan, T. S. (2002). Removal of mercury(II) from aqueous solutions and chlor-alkali industry wastewater using 2-mercaptobenzimidazole-clay. *Water Research, 36,* 1609–1619. https://doi.org/10.1016/S0043-1354(01)00362-1

Martell, A.E. & Smith, R.M. (1977). *Critical Stability Constants* (Plenum press.). New York.

Martell, A.E., Smith, R.M., & Motekaitis, R.J. (2004). *NIST Standard Reference Database 46, vers.8*. Gaithersburg, MD, USA.

Massaro, M., Riela, S., Guernelli, S., Parisi, F., Lazzara, G., Baschieri, A., et al. (2016). A synergic nanoantioxidant based on covalently modified halloysite–trolox nanotubes with intra-lumen loaded quercetin. *Journal of Materials Chemistry B, 4,* 2229–2241. https://doi.org/10.1039/C6TB00126B

Massaro, M., Colletti, C. G., Buscemi, G., Cataldo, S., Guernelli, S., Lazzara, G., et al. (2018). Palladium nanoparticles immobilized on halloysite nanotubes covered by a multilayer network for catalytic applications. *New Journal of Chemistry, 42,* 13938–13947. https://doi.org/10.1039/C8NJ02932F

Massaro, M., Colletti, C. G., Fiore, B., Parola, V. L., Lazzara, G., Guernelli, S., et al. (2019). Gold nanoparticles stabilized by modified halloysite nanotubes for catalytic applications. *Applied Organometallic Chemistry, 33,* e4665. https://doi.org/10.1002/aoc.4665

Massaro, M., Casiello, M., D'Accolti, L., Lazzara, G., Nacci, A., Nicotra, G., et al. (2020). One-pot synthesis of ZnO nanoparticles supported on halloysite nanotubes for catalytic applications. *Applied Clay Science, 189,* 105527. https://doi.org/10.1016/j.clay.2020.105527

Onal, Y., Akmil-Başar, C., & Sarici-Ozdemir, C. (2007). Elucidation of the naproxen sodium adsorption onto activated carbon prepared from waste apricot: kinetic, equilibrium and thermodynamic characterization. *Journal of Hazardous Materials, 148,* 727–734. https://doi.org/10.1016/j.jhazmat.2007.03.037

Owoseni, O., Nyankson, E., Zhang, Y., Adams, S. J., He, J., McPherson, G. L., et al. (2014). Release of surfactant cargo from interfacially-active halloysite clay nanotubes for oil spill remediation. *Langmuir, 30,* 13533–13541. https://doi.org/10.1021/la503687b

Peng, Q., Liu, M., Zheng, J., & Zhou, C. (2015). Adsorption of dyes in aqueous solutions by chitosan–halloysite nanotubes composite hydrogel beads. *Microporous and Mesoporous Materials, 201,* 190–201. https://doi.org/10.1016/j.micromeso.2014.09.003

Renu, A. M., & Singh, K. (2017). Heavy metal removal from wastewater using various adsorbents: a review. *Journal of Water Reuse and Desalination, 7,* 387–419. https://doi.org/10.2166/wrd.2016.104.

Tran, H. N., You, S.-J., & Chao, H.-P. (2016). Thermodynamic parameters of cadmium adsorption onto orange peel calculated from various methods: A comparison study. *Journal of Environmental Chemical Engineering, 4,* 2671–2682. https://doi.org/10.1016/j.jece.2016.05.009

Uddin, M. K. (2017). A review on the adsorption of heavy metals by clay minerals, with special focus on the past decade. *Chemical Engineering Journal, 308,* 438–462. https://doi.org/10.1016/j.cej.2016.09.029

UN Environment. (2019). (Global Mercury Assessment 2018. UN Environment Programme, Chemicals and Health Branch Geneva, Switzerland). Retrieved from http://www.unenvironment.org/resources/publication/global-mercury-assessment-20182018

Von Burg, R., & Greenwood, M.R. (1991). Mercury. Pp. 1045–1089 in: *Metals and their Compounds in the Environment: Occurrence, Analysis, and Biological Relevance*. (E. Merian, editor). VCH, Weinheim, Germany.

Walcarius, A., & Delacôte, C. (2005). Mercury(II) binding to thiol-functionalized mesoporous silicas: Critical effect of pH and sorbent properties on capacity and selectivity. *Analytica Chimica Acta, 547,* 3–13. https://doi.org/10.1016/j.aca.2004.11.047

Wang, Q., Kim, D., Dionysiou, D. D., Sorial, G. A., & Timberlake, D. (2004). Sources and remediation for mercury contamination in aquatic systems – A literature review. *Environmental Pollution, 131,* 323–336. https://doi.org/10.1016/j.envpol.2004.01.010

Wei, W., Minullina, R., Abdullayev, E., Fakhrullin, R., Mills, D., & Lvov, Y. (2013). Enhanced efficiency of antiseptics with sustained release from clay nanotubes. *RSC Advances, 4,* 488–494. https://doi.org/10.1039/C3RA45011B

Ynalvez, R., Gutierrez, J., & Gonzalez-Cantu, H. (2016). Mini-review: Toxicity of mercury as a consequence of enzyme alteration. *BioMetals, 29,* 781–788. https://doi.org/10.1007/s10534-016-9967-8

(Received 26 May 2020; revised 26 January 2021; AE: Deb P. Jaisi)